Hyperspectral Unmixing via Convolutional Neural Network

Kemal Gürkan Toker[1], Seniha Esen Yüksel[2]

[1]Tubitak Bilgem ILTAREN, Ankara, TURKEY
gurkan.toker@tubitak.gov.tr

[2]Graduate School of Science and Engineering, Department of Electrical and Electronics Engineering, Hacettepe University, Ankara, TURKEY

eyuksel@ee.hacettepe.edu.tr

Abstract — *Hyperspectral imaging sensors provide image data containing both spatial and detailed spectral information. However, due to the low spatial resolution or to the presence of intimate mixtures in the scene, the spectral information acquired by the hyperspectral sensors are actually mixtures of the spectral signatures of the materials. These mixtures are modelled as linear or nonlinear in the literature. In this study, convolutional neural network is proposed for linear hyperspectral unmixing. The spectral signatures of some materials, taken from the ASTER and USGS spectral libraries, are used to construct a specific library to be used in the experiments. These signatures in the constructed library are used to obtain synthetic mixture pixels within the framework of the linear mixture model. These mixture pixels are used for training a convolutional neural network. The trained convolutional neural network is used for determining (i) which materials in the library are included in mixed pixels and (ii) their corresponding fractional abundances that best model each mixed test pixel. Also, the effects of the number of training data and the level of noise on unmixing performance are investigated. It has been shown that promising unmixing results have been achieved by using the convolutional neural network.*

Keywords: *Hyperspectral imaging, unmixing, convolutional neural network*

1 Introduction

During recent years, convolutional neural network has been gaining a large amount of interest in various vision-related tasks such as scene labeling [1], digit classification [2], character classification [3], face recognition [4]. Besides vision tasks, CNNs have been demonstrated to be successful in other areas as well, such as speech recognition [5] and natural language processing [6]. In this study, convolutional neural network is proposed for hyperspectral unmixing.

Hyperspectral imaging sensors provide image data containing both spatial and detailed spectral information [7]. However, due to low spatial resolution of the sensors or to the presence of intimate mixtures in the scene, the spectral information acquired by the hyperspectral sensors are actually mixtures of the spectral signatures of the materials [8]. The mixtures are modelled as linear or nonlinear in the literature. In this study, we focus on the linear mixing model. In linear spectral unmixing, the aim is to decompose the measured spectrum of a mixed pixel into reference spectral signatures of the materials, also called endmember (estimating endmembers), and estimate a set of corresponding fractions, also called abundances that indicate the proportion of each endmember present in the pixel (estimating corresponding abundances)[9]. For p endmembers, each having L bands, the linear mixing model is expressed as:

$$y = \sum_{i=1}^{p} a_i m_i + w = M\alpha + w \tag{1}$$

where y is the $L \times 1$ pixel spectrum vector received by sensor, M is the $L \times p$ matrix whose columns are the $L \times 1$ endmembers m_i; a is the $p \times 1$ fractional abundance vector consisting of a_i, i, =$1 \ldots p$ and w is the $L \times 1$ additive perturbation vector (noise and modeling errors). The fractional abundances are subject to the following constraints:

$$a_i \geq 0, i = 1 \ldots p \tag{2}$$
$$\sum_{i=1}^{p} a_i = 1$$

The constraints are termed as the abundance nonnegativity constraint (ANC) and the abundance sum constraint (ASC) respectively.

Linear spectral unmixing has been extensively researched in the recent years. Many methods have been developed for this problem. Most of these methods are geometrical or statistical based approaches. In geometrical based approaches, some methods make an assumption for endmember extraction that there is at least one pure pixel in the scene [10] [11] [12]. However, this assumption cannot be always guaranteed. Some of the other spectral unmixing methods do not make the pure pixel assumption for endmember extraction [13] [14] [15] [16]. However, these methods generate endmember signatures which are often not associated with the real physical signatures [8] [9] [17]. In addition, results obtained by these geometrical based methods are unsatisfactory when the spectral mixtures are highly mixed. In these cases, statistical methods are used as an alternative [18] [19]. On the other hand, statistical methods have higher computational complexity in comparison with geometrical based methods [20]. These drawbacks and limitations have led to the use of spectral libraries instead of endmember estimation. When using libraries, the observed mixed pixel can be expressed as linear combinations of a number of pure spectral signatures which are taken from library. Thus, unmixing is equivalent to determining which materials in the library are included in mixed pixels and their corresponding fractional abundances that can best model each mixed pixel in the scene. Hence, sparse regression based methods has been developed for hyperspectral unmixing [21] [22] [23].

In this paper, a convolutional neural network is proposed to determine which materials in the library are included in mixed pixels and their corresponding fractional abundances that can best model each mixed test pixel. Also, the effects of the number of training data and the level of noise on unmixing performance are investigated on synthetic hyperspectral data. This paper is organized as follows: in section 2 the proposed CNN architecture for hyperspectral unmixing is introduced. In section 3 the experiments using the synthetic data are explained. In section 4 the paper is concluded with our remarks.

2 Proposed CNN Architecture

In this study, convolutional neural network is proposed for hyperspectral unmixing. Convolutional neural network structure which contains two convolutional layer and a fully connected layer is used in the experiments. CNN is directly applied on the spectral domain.

The proposed CNN architecture (the layers, the number of filter sizes and number of filters) is given in Figure 1. Fixed learning rate which is equal to 0.01, is used. The stopping condition for the CNN model is the fixed iteration number which is set to 2000. Our experiments have shown that this is a large enough number to garantee convergence. Stochastic gradient descent is used as a learning method and cross entropy is used as a cost function. All the programs are implemented using Python language and Tensorflow [24] library.

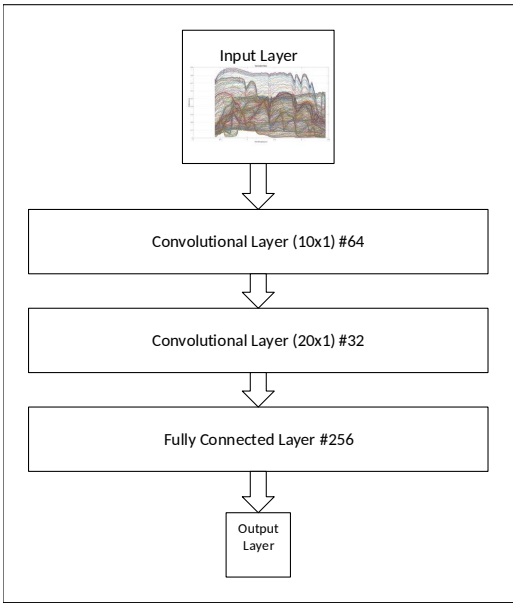

Figure 1: The proposed CNN architecture: input represents a pixel spectral vector, followed by 2 convolution layers, a fully connected layer and finally the output layer.

The mean estimation error is used to evaluate the abundance estimations. The error is defined as:

$$\text{Mean Estimation Error} = \frac{1}{n}\frac{1}{k}\sum_{i=1}^{n}\Big[\sum_{j=1}^{k}[a_{ij} - \hat{a}_{ij}]\Big] \tag{3}$$

where n is the number of test data which is equal to 200 and k is the number of endmembers which is equal to 12 in our experiments. Also, $\hat{a}$ is the estimated abundances by the network. Generally speaking, the smaller mean estimation error is, the more the estimation approximates the truth.

3 Experiments on Synthetic Hyperspectral Data

3.1 Synthetic Data

The spectral libraries ASTER [25] (Advanced Spaceborne Thermal Emission and Reflection Radiometer) and USGS [26] (United States Geological Survey) are used in our experiments. The spectral signatures of some materials, taken from ASTER and USGS spectral libraries, are used to construct specific library to be used in the experiments. The spectral signatures of these materials are taken at different wavelengths and they have different spectral resolutions. Therefore, preprocessing is performed at the beginning of the experiments. For each material, spectral information between 0.4 and 2.45 micrometers is taken into account and is extrapolated to 281 bands. The experiments were performed with a subset library composed of 12 materials chosen from the spectral libraries. To obtain synthetic mixture pixels, first of all, the endmember matrix M is generated using these selected material signatures. Then, the matrix of fractional abundances, which satisfies the constraints in Equation 2, are obtained using the Dirichlet distribution. These signatures in the constructed library and the fractional abundances are used to obtain synthetic mixture pixels within the framework of the linear mixture model as given in Equation 1.

The first synthetic hyperspectral training data set contains 1000 pixels randomly generated following a Dirichlet distribution. The signatures of these materials and the spectral information of 1000 mixture pixels are shown in Figure 2. These 1000 mixture pixels are used as training data.

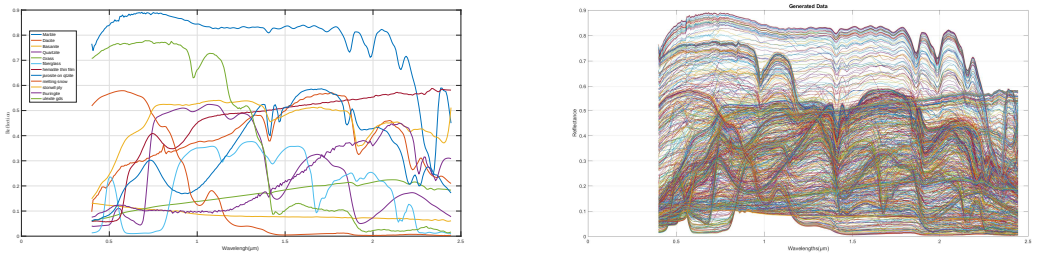

(a) Spectral signatures of 12 materials

(b) Spectral information of mixture pixel

Figure 2: Spectral signatures of 12 materials taken from the ASTER and USGS datasets which are used in the experiments and 1000 mixture pixels produced from selected these 12 spectral signatures.

For the second synthetic hyperspectral training data, the abundances are generated in the same way as the first synthetic data. But, this time 10000 mixture pixels are generated randomly to investigate the effects of training data on the unmixing performance. The 200 test data is also generated in the same way.

3.2 Results

The generated mixture pixels are used as training data and the corresponding fractional abundances at each pixel are used as labels to train the convolutional neural network that is presented in Section 2. The trained neural network is used to find which signatures are in the mixed test pixel and estimate the corresponding fractional abundances in the 200 test pixels. The error values between real abundances and the estimated abundances are calculated using Equation 3. This error measures the average errors, that is, the difference between real and estimated abundances. The mean estimation errors of each structure are given in Table 1.

Number of training data	Mean Estimation Error
1000	0.0248
10000	0.0218

Table 1: The mean estimation errors of each structure

The estimation performances of the 20 test data are visualized with Hinton diagrams in Figure 3. Hinton diagrams are a way of visualizing numerical values in a matrix/vector and are used in the neural networks and machine learning literature. The size of each square in the diagram represents the magnitude of each value. In Figure 3, each row indicates the samples of 20 test data and each column indicates the real and estimated fractional abundances of the samples.

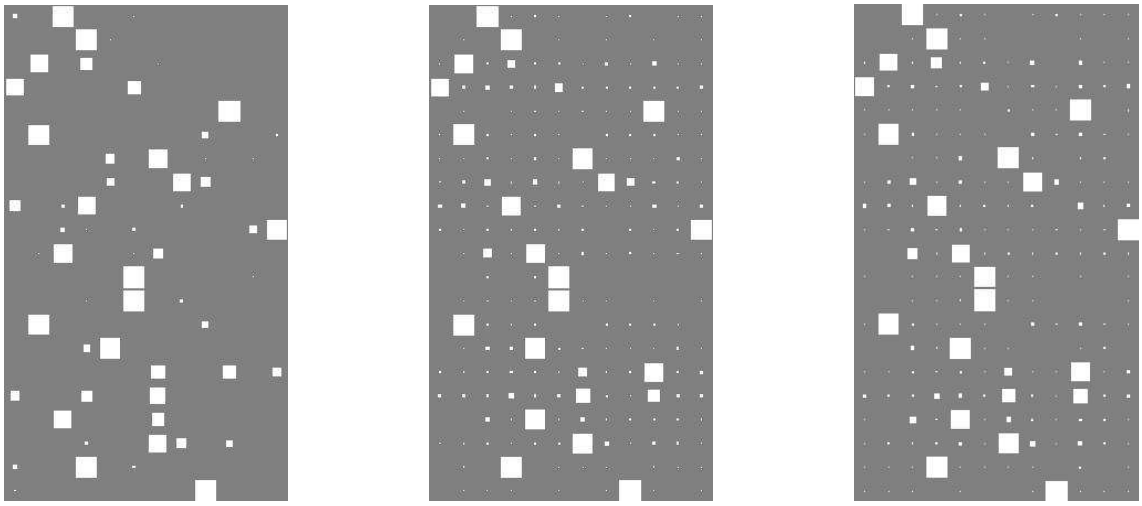

(a) Real fractional abundances

(b) Estimated abundances with 1000 training data

(c) Estimated abundances with 10000 training data

Figure 3: Hinton diagrams of real and estimated fractional abundances

It is seen from Figure 3 that the fractional abundances, which should actually be zero, is suppressed and forced to be nearly zero when the convolutional neural network is used.

But they are not exactly zero. This causes errors. Besides, the large fractional abundances can be estimated correctly for the most part for each neural networks. This means dominant materials can be found in the mixture pixels.

In order to examine the effects of noise on the unmixing performance of network, the synthetic training data sets are contaminated by Gaussian white noise with two levels of SNR: 30 and 40 dB. Network is trained using this noisy training data. The purpose of this experiment is to examine how the performance of networks may be affected if there are differences between the spectral information in the hyperspectral image taken in real life and the spectral signatures in the library. The mean estimation errors of the network for noisy data are given in Table 2.

Number of training data	Noise Level	Mean Estimation Error
1000	30 dB	0.0295
	40 dB	0.0264
	No Noise	0.0248
10000	30 dB	0.0244
	40 dB	0.0226
	No Noise	0.0218

Table 2: The mean estimation errors of each structure

As the noise gets stronger, the performances of the trained networks reduces. Also, it can be seen that the network trained with 10000 training data behaves better than the other one.

4 Conclusion

In this study, convolutional neural network is proposed for linear hyperspectral unmixing and it is shown that CNNs are a good way to solve unmixig problems. The the effects of the number of training data and the level of noise on unmixing performance is examined. It is observed that with the increase of training data, the estimation performance of fractional abundances also increases. Convolutional neural network is less affected by the increased level of noise with the increase of training data. It has been shown that promising unmixing results have been achieved using convolutional neural network.

In the future, we plan to analyze unmixing performance of the convolutional neural network on real data and compare the performance of the method with sparse regression based methods. In this study, 12 signatures were taken from the spectral library to construct a subset library. In the future, we plan to obtain mixture pixels by taking a larger size of material signatures from the library and to examine the performance of convolutional neural network on them.

References

[1] Clement Farabet, Camille Couprie, Laurent Najman, and Yann LeCun. Learning hierarchical features for scene labeling. *IEEE transactions on pattern analysis and machine intelligence*, 35(8):1915–1929, 2013.

[2] Pierre Sermanet, Soumith Chintala, and Yann LeCun. Convolutional neural networks applied to house numbers digit classification. In *Pattern Recognition (ICPR), 2012 21st International Conference on*, pages 3288–3291. IEEE, 2012.

[3] Dan Claudiu Ciresan, Ueli Meier, Luca Maria Gambardella, and Jurgen Schmidhuber. Convolutional neural network committees for handwritten character classification. In *Document Analysis and Recognition (ICDAR), 2011 International Conference on*, pages 1135–1139. IEEE, 2011.

[4] Steve Lawrence, C Lee Giles, Ah Chung Tsoi, and Andrew D Back. Face recognition: A convolutional neural-network approach. *IEEE transactions on neural networks*, 8(1):98–113, 1997.

[5] Ossama Abdel-Hamid, Abdel-rahman Mohamed, Hui Jiang, and Gerald Penn. Applying convolutional neural networks concepts to hybrid nn-hmm model for speech recognition. In *Acoustics, Speech and Signal Processing (ICASSP), 2012 IEEE International Conference on*, pages 4277–4280. IEEE, 2012.

[6] Nal Kalchbrenner, Edward Grefenstette, and Phil Blunsom. A convolutional neural network for modelling sentences. *arXiv preprint arXiv:1404.2188*, 2014.

[7] J. Bioucas-Dias, A. Plaza, G. Camps-Valls, N. Nasrabadi, P. Scheunders, and J. Chanussot. Hyperspectral remote sensing data analysis and future challenges. *IEEE Geoscience and Remote Sensing Magazine*, 1(2):6–36, June 2013.

[8] J. Bioucas-Dias, A. Plaza, Dobigeon, Parente, Qian Du Du, Gader, and J. Chanussot. Hyperspectral unmixing overview: geometrical, statistical, and sparse regression-based approaches. *IEEE Journal of Selected Topics in Applied Earth Observations and Remote Sensing*, 5(2):354–370, April 2012.

[9] N. Keshava and J. F. Mustard. Spectral unmixing. *IEEE Signal Processing Magazine*, 19(1):44–57, Jan 2002.

[10] Michael E Winter. N-findr: An algorithm for fast autonomous spectral end-member determination in hyperspectral data. In *SPIE's International Symposium on Optical Science, Engineering, and Instrumentation*, pages 266–275. International Society for Optics and Photonics, 1999.

[11] T Szeredi J Lefevbre R.A Neville, K Staenz and P Hauff. Automatic endmember extraction from hyperspectral data for mineral exploration. In *International Airborne Remote Sensing Conference and Exhibition, 4 th/21 st Canadian Symposium on Remote Sensing*, 1999.

[12] J. M. P. Nascimento and J. M. B. Dias. Vertex component analysis: a fast algorithm to unmix hyperspectral data. *IEEE Transactions on Geoscience and Remote Sensing*, 43(4):898–910, April 2005.

[13] M. Berman, H. Kiiveri, R. Lagerstrom, A. Ernst, R. Dunne, and J. F. Huntington. Ice: a statistical approach to identifying endmembers in hyperspectral images. *IEEE Transactions on Geoscience and Remote Sensing*, 42(10):2085–2095, Oct 2004.

[14] Alina Zare and Paul Gader. Spice: A sparsity promoting iterated constrained endmember extraction algorithm with applications to landmine detection from hyperspectral imagery. In *Defense and Security Symposium*, pages 655319–655319. International Society for Optics and Photonics, 2007.

[15] J. Li and J. Bioucas-Dias. Minimum volume simplex analysis: a fast algorithm to unmix hyperspectral data. In *IEEE International Geoscience and Remote Sensing Symp.- IGARSS*, volume 1, pages 1–4, July 2008.

[16] Seniha Esen Yuksel, Sefa Kucuk, and Paul D Gader. Spicee: An extension of spice for sparse endmember estimation in hyperspectral imagery. *IEEE Geoscience and Remote Sensing Letters*, 13(12):1910–1914, 2016.

[17] W. K. Ma, J. M. Bioucas-Dias, T. H. Chan, N. Gillis, P. Gader, A. J. Plaza, A. Ambikapathi, and C. Y. Chi. A signal processing perspective on hyperspectral unmixing: Insights from remote sensing. *IEEE Signal Processing Magazine*, 31(1):67–81, Jan 2014.

[18] Nicolas Dobigeon, Saïd Moussaoui, Martial Coulon, Jean-Yves Tourneret, and Alfred O Hero. Joint bayesian endmember extraction and linear unmixing for hyperspectral imagery. *IEEE Transactions on Signal Processing*, 57(11):4355–4368, 2009.

[19] José MP Nascimento and José M Bioucas-Dias. Hyperspectral unmixing based on mixtures of dirichlet components. *IEEE Transactions on Geoscience and Remote Sensing*, 50(3):863–878, 2012.

[20] José M Bioucas-Dias and Antonio Plaza. An overview on hyperspectral unmixing: Geometrical, statistical, and sparse regression based approaches. In *Geoscience and Remote Sensing Symposium (IGARSS), 2011 IEEE International*, pages 1135–1138. IEEE, 2011.

[21] Marian-Daniel Iordache, José M Bioucas-Dias, and Antonio Plaza. Sparse unmixing of hyperspectral data. *IEEE Transactions on Geoscience and Remote Sensing*, 49(6):2014–2039, 2011.

[22] Wei Tang, Zhenwei Shi, Ying Wu, and Changshui Zhang. Sparse unmixing of hyperspectral data using spectral a priori information. *IEEE Transactions on Geoscience and Remote Sensing*, 53(2):770–783, 2015.

[23] Yang Guo, Tai Gao, Chengzhi Deng, Shengqian Wang, and JianPing Xiao. Sparse unmixing using an approximate l0 regularization. In *First International Conference on Information Sciences, Machinery, Materials and Energy*. Atlantis Press, 2015.

[24] Martín Abadi, Ashish Agarwal, Paul Barham, Eugene Brevdo, Zhifeng Chen, Craig Citro, Greg S. Corrado, Andy Davis, Jeffrey Dean, Matthieu Devin, Sanjay Ghemawat, Ian Goodfellow, Andrew Harp, Geoffrey Irving, Michael Isard, Yangqing Jia, Rafal Jozefowicz, Lukasz Kaiser, Manjunath Kudlur, Josh Levenberg, Dan Mané, Rajat Monga, Sherry Moore, Derek Murray, Chris Olah, Mike Schuster, Jonathon Shlens, Benoit Steiner, Ilya Sutskever, Kunal Talwar, Paul Tucker, Vincent Vanhoucke, Vijay Vasudevan, Fernanda Viégas, Oriol Vinyals, Pete Warden, Martin Wattenberg, Martin Wicke, Yuan Yu, and Xiaoqiang Zheng. TensorFlow: Large-scale machine learning on heterogeneous systems, 2015. Software available from tensorflow.org.

[25] AM Baldridge, SJ Hook, CI Grove, and G Rivera. The aster spectral library version 2.0. *Remote Sensing of Environment*, 113(4):711–715, 2009.

[26] R.N. Clark, G.A. Swayze, R. Wise, E. Livo, T. Hoefen, R. Kokaly, and S.J Sutley. Usgs digital spectral library splib06a: U.s. geological survey, digital data series 231. http://speclab.cr.usgs.gov/spectral.lib06, 2007. Accessed March 6, 2017.